

Semianalytical solution of the Kondo model in a magnetic field

C. Slezak,^{1,2} S. Kehrein,¹ Th. Pruschke,¹ and M. Jarrell²¹*Center for Electronic Correlations and Magnetism, Theoretical Physics III, Institute for Physics, University of Augsburg, 86135 Augsburg, Germany*²*Department of Physics, University of Cincinnati, Cincinnati, Ohio 45221*

(Received 28 August 2002; revised manuscript received 20 December 2002; published 8 May 2003)

The single impurity Kondo model at zero temperature in a magnetic field is solved by an approximate semianalytical approach based on the flow-equation method. The resulting problem is shown to be equivalent to a resonant-level model with a nonconstant hybridization function. This nontrivial *effective hybridization function* encodes the quasiparticle interaction in the Kondo limit, while the magnetic field enters as the impurity orbital energy. The evaluation of static and dynamic quantities of the strong-coupling Kondo model becomes very simple in this effective model. We present results for thermodynamic quantities and the dynamical spin-structure factor and compare them with numerical renormalization-group calculations.

DOI: 10.1103/PhysRevB.67.184408

PACS number(s): 72.15.Qm, 75.20.Hr, 71.27.+a

I. INTRODUCTION

The single impurity Kondo model (SIKM) or *s-d* model¹

$$H_{\text{SIKM}} = \sum_{k\sigma} \epsilon_{\vec{k}} c_{k\sigma}^\dagger c_{\vec{k}\sigma} + J \sum_{\vec{k}\vec{k}'} \sum_{\alpha\beta} c_{k\alpha}^\dagger \vec{S} \cdot \vec{\sigma}_{\alpha\beta} c_{\vec{k}'\beta} \quad (1)$$

is, together with its close relative, the single impurity Anderson model,² one of the fundamental models in the theory of correlated electron systems. It has been studied extensively over the past four decades,³ but despite its simplicity, no complete analytic solution exists that provides information on both thermodynamic and dynamical quantities. For example, the Bethe ansatz solution^{3,4} has solved all universal properties of the Kondo problem including its high- to low-temperature crossover behavior. But the Bethe ansatz requires the limit of infinite conduction bandwidth and cannot be used to calculate dynamical quantities beyond the low-energy limit.

Thus, numerical methods, like Wilson's numerical renormalization group^{3,5} (NRG) or quantum Monte Carlo (QMC),⁶ in connection with maximum-entropy methods,⁷ have to be employed to access dynamical quantities on all energy scales. In both methods, evaluation of dynamical properties, and quantities related to them, such as the Korrington-Shiba relation or the Friedel sum rule,³ suffer from unavoidable numerical errors. QMC simulations, in addition, cannot be used at zero temperature and are restricted to comparatively large values of J .⁶ Moreover, a reliable evaluation of single- and two-particle spectra and related quantities in an external magnetic field, as well as their comparison and interpretation within a local Fermi-liquid picture,³ become rather problematic,^{8,9} especially in the limit of vanishing external magnetic field. Approximate analytical techniques, such as perturbation expansions or $1/N$ expansions,³ typically only describe certain properties of the Kondo model correctly. A notable exception in this respect is the so-called local-moment approach.¹⁰ This perturbative approach is very accurate in most cases,¹¹ including those of nonvanishing external magnetic fields.^{9,12}

Besides its relevance for the study of moment formation in metals, the Kondo model (1) has gained new importance as input for investigating nondilute correlated electron systems such as heavy fermion materials within dynamical mean-field theory (DMFT).¹³ Here a reliable method for calculating single-particle correlation functions, especially close to the Fermi energy, is extremely important.

In this paper, we propose a new *nonperturbative* semianalytical approach to the Kondo problem based on Wegner's flow-equation method¹⁴ and previous work on applications of flow equations to strong-coupling problems.^{15,16} We will show that to a very good approximation, many physical quantities of the Kondo model in the small coupling limit ($\rho_0 J \rightarrow 0$) can be calculated from a resonant-level model, where the interacting features of the Kondo model are encoded in a nonconstant *effective hybridization function* of this resonant-level model. Thereby we extend the well-known strong-coupling result by Toulouse¹⁷ that the Kondo model on the Toulouse line is equivalent to a resonant-level model with a flat hybridization function. Surprisingly, even in the small coupling limit (Kondo limit) our noninteracting effective model describes both universal low-energy properties such as the Wilson ratio as well as high-energy power laws and logarithmic corrections with very good accuracy. Due to the noninteracting nature of this effective model this mapping allows immediate insight into the physics of the Kondo model, for example, the dependence of its static and dynamical quantities on a local magnetic field.

After presenting our approach in the next section, we discuss several static quantities at $T=0$ as a function of a local magnetic field and derive analytical expressions for their asymptotic behavior. As an example for a dynamical quantity, we then discuss the spin-structure factor and the Korrington-Shiba relation. An outlook on potential future applications of our approach concludes this paper.

II. MAPPING TO A RESONANT-LEVEL MODEL

A. Principles of the flow-equation method

The general framework of the flow-equation method¹⁴ and its application to the Kondo model has been explained in

detail in Ref. 16. Here we will only repeat the main steps in order to make this paper self-contained, and refer to Ref. 16 for more details.

The key idea of the flow-equation approach consists of performing a continuous sequence of infinitesimal unitary transformations on a given Hamiltonian,

$$\frac{dH(B)}{dB} = [\eta(B), H(B)]. \quad (2)$$

With an anti-Hermitian generator $\eta(B)$ the solution of Eq. (2) describes a family of unitarily equivalent Hamiltonians $H(B)$ parametrized by the flow parameter B . By choosing $\eta(B)$ appropriately¹⁴ one can set up a framework that diagonalizes a many-particle Hamiltonian $H(B=0)$, i.e., $H(B=\infty)$ becomes diagonal.

The concrete realization of this approach for the Kondo model was discussed in Ref. 16. The starting point is the bosonized form¹⁸ of the Hamiltonian (1). Since we are mainly interested in describing the basic ideas of our approach, we restrict ourselves to a linear dispersion relation. Notice, however, that the flow-equation approach can also be used for a nontrivial conduction-band density of states since it does not rely on the integrability of the model.¹⁹ With a linear dispersion relation the Kondo problem becomes effectively one dimensional, the charge-density excitations in Eq. (1) decouple, and we only need to look at the spin-density part,

$$H = H_0 - \frac{J}{\sqrt{8\pi^2}} \partial_x \Phi(0) S^z + \frac{J}{4\pi a} [e^{i\sqrt{2}\Phi(0)} S^- + \text{H.c.}] \quad (3)$$

with $H_0 = \sum_{q>0} q \sigma(q) \sigma(-q)$. Here $\sigma(p) = 1/\sqrt{2|p|} [\sum_q (c_{p+q}^\dagger c_{q\uparrow} - c_{p+q}^\dagger c_{q\downarrow})]$ are the bosonic spin-density modes with the bosonic spin-density field defined by $\Phi(x) = -i \sum_{q \neq 0} \sqrt{|q|} / |q| e^{-iqx-a|q|/2} \sigma(q)$. For simplicity we have set the Fermi velocity $v_F = 1$. a is proportional to the inverse conduction bandwidth. All our latter results will be expressed as universal functions of the low-energy Kondo scale T_K , and we can consider Eq. (3) to be equivalent to our original Kondo Hamiltonian if $T_K \ll a^{-1}$.

Equation (3) was used as the starting point $H(B=0)$ of the flow-equation approach in Ref. 16. Away from the Toulouse point the unitary equivalence of the flow holds only approximately, but this approximation can be controlled by a small parameter¹⁵ and yields very accurate results. During the flow the Hamiltonian can be parametrized as

$$H(B) = H_0 + \sum_p g_p(B) (C_p^\dagger[\lambda(B)] S^- + \text{H.c.}) + \sum_p \omega_p(B) \{C_p^\dagger[\lambda(B_p)], C_p[\lambda(B_p)]\}. \quad (4)$$

Here $B_p = p^{-2}$, and $C_p^\dagger(\lambda)$, $C_p(\lambda)$ denote normalized vertex operators with scaling dimension $\lambda > 0$ in momentum space,

$$C_p^\dagger(\lambda) \stackrel{\text{def}}{=} \left[\frac{\Gamma(\lambda^2)}{2\pi a L} \right]^{1/2} |pa|^{(1-\lambda^2)/2} \int_{-L/2}^{L/2} dx e^{ipx + i\lambda\Phi(x)},$$

$$C_p(\lambda) \stackrel{\text{def}}{=} \left[\frac{\Gamma(\lambda^2)}{2\pi a L} \right]^{1/2} |pa|^{(1-\lambda^2)/2} \int_{-L/2}^{L/2} dx e^{-ipx - i\lambda\Phi(x)}$$

that obey $\langle \Omega | C_p(\lambda) C_{p'}^\dagger(\lambda) | \Omega \rangle = \delta_{pp'}$ and $\langle \Omega | C_p^\dagger(\lambda) C_{p'}(\lambda) | \Omega \rangle = \delta_{pp'}$. For the special case $\lambda = 1$ they fulfill fermionic anticommutation relations $\{C_p^\dagger(1), C_{p'}(1)\} = \delta_{pp'}$ and can therefore be interpreted as creation and annihilation operators for fermions.

In Ref. 16 the following flow equations for the parameters in Eq. (4) have been derived:

$$\begin{aligned} \frac{dg_p}{dB} &= -p^2 g_p + \frac{2\pi}{\Gamma(\lambda^2)} \sum_{q \neq p} \frac{p+q}{p-q} g_p g_q^2 |qa|^{\lambda^2-1} \\ &+ \frac{1}{4} g_p \ln(B/a^2) \frac{d\lambda^2}{dB}, \end{aligned} \quad (5)$$

$$\frac{d\omega_q}{dB} = \frac{2\pi}{\Gamma(\lambda^2)} q g_q^2 |qa|^{\lambda^2-1} \quad (6)$$

and the following is the differential equation for the flow of the scaling dimension:

$$\frac{d\lambda^2}{dB} = \frac{8\pi\lambda^2(1-\lambda^2)}{\Gamma(\lambda^2)} \sum_q g_q g_{-q} |qa|^{\lambda^2-1}. \quad (7)$$

It can be shown¹⁶ that one always finds $\lambda \rightarrow 1$ in the strong-coupling phase of the Kondo model, i.e., in the low-energy limit the vertex operators in Eq. (4) become fermions. In the following we will use an improved version of the above flow equations by taking into account that all approximations should be performed with respect to the interacting ground state: It turns out that the only necessary modification in Eqs. (5)–(7) is that the exponent in $|qa|^{\lambda^2-1}$ gets replaced by $\lambda^2(B_q) - 1$, i.e., it is no longer a running exponent.²⁰

B. Equivalence to a resonant-level model

Now we will compare this system of differential equations with the flow equations for a resonant-level model. This will lead to the *key result* of this paper: the resonant-level model can be used as an *effective model* for the complicated strong-coupling Kondo model.

The Hamiltonian of the resonant-level model (RLM) is given by

$$H_{\text{RLM}} = \sum_k \epsilon_k c_k^\dagger c_k + \epsilon_d d^\dagger d + \sum_k V_k (c_k^\dagger d + d^\dagger c_k). \quad (8)$$

Following the same flow-equation approach as previously used in the Kondo model, we establish a solution to the resonant-level model (8). A detailed description of the flow-equation solution can be found in Ref. 21. One finds the following flow equations for the parameters in Eq. (8):

$$\frac{dV_k}{dB} = -V_k(\epsilon_d - \epsilon_k)^2 + \sum_{q \neq k} V_k V_q^2 \frac{\epsilon_k + \epsilon_q - 2\epsilon_d}{\epsilon_k - \epsilon_q}, \quad (9)$$

$$\frac{d\epsilon_d}{dB} = -2 \sum_k V_k^2 (\epsilon_k - \epsilon_d), \quad (10)$$

$$\frac{d\epsilon_k}{dB} = 2V_k^2 (\epsilon_k - \epsilon_d). \quad (11)$$

It should be noted that this yields the exact analytical solution. Having established the flow equations to solve both the Kondo model and the resonant-level model, respectively, one can now show an approximate equivalence of these two models. We introduce the substitution

$$V_k^2 = \frac{2\pi}{\Gamma[\lambda^2(B_k)]} g_k^2 |ka|^{\lambda^2(B_k)-1} \quad (12)$$

and notice that with this substitution the two sets of flow equations, Eqs. (5) and (6) and (9)–(11), become equivalent for $\epsilon_d = 0$ in the resonant-level model, with the exception of the logarithmic term in Eq. (5). Thus we now have established an approximate mapping of the Kondo model onto the resonant-level model by means of Eq. (12) in the sense that their flow-equation diagonalization is identical. We shall refer to this relation by introducing the *effective hybridization function* $\Delta_{\text{eff}}(\epsilon) = \pi \sum_k V_k^2 \delta(\epsilon - \epsilon_k)$: the resonant-level model with this nontrivial hybridization function can be used as an effective model for the Kondo model in the Kondo limit (small coupling limit) $\rho_0 J \rightarrow 0$. Since this noninteracting resonant-level model is a simple, quadratic Hamiltonian, this mapping will allow us to read off and understand many properties of the complicated many-body Kondo physics in an intuitive and straightforward way. It will turn out that the deviations of $\Delta_{\text{eff}}(\epsilon)$ from a constant hybridization function encode the quasiparticle interaction and therefore the many-body Kondo physics in this quadratic effective Hamiltonian.

Notice that the above mapping between the Kondo model and the resonant-level model becomes *exact* at the Toulouse point¹⁷ $\rho_0 J = 2\pi(2 - \sqrt{2})$ since $\lambda^2(B) = 1$ for all flow parameters B . One easily verifies that the effective resonant-level model then has a constant hybridization function, $\Delta_{\text{eff}}(\epsilon) = (\pi/4)\rho_0 J^2$. In this case, our mapping just reduces to the observation already made by Toulouse that the partition function of the Kondo model for this specific coupling constant J is exactly equivalent to the partition function of a quadratic Hamiltonian.¹⁷

In order to specify the function $\Delta_{\text{eff}}(\epsilon)$ in the Kondo limit it is best to not directly use relation (12), but to determine the effective hybridization function from matching a correlation function in the Kondo model and the resonant-level model. We have chosen the $\langle S^+(t)S^-(0) \rangle$ correlation function, evaluated it with respect to Eq. (4) for $B = 0$, and then chose $\Delta_{\text{eff}}(\epsilon)$ in the resonant-level model such that this coincided with the $\langle d^\dagger(t)d(0) \rangle$ correlation function. The resulting $\Delta_{\text{eff}}(\epsilon)$ agrees with Eq. (12) in the high- and low-energy regimes, with deviations only in the crossover region. However, the mapping from the Kondo model to the effective

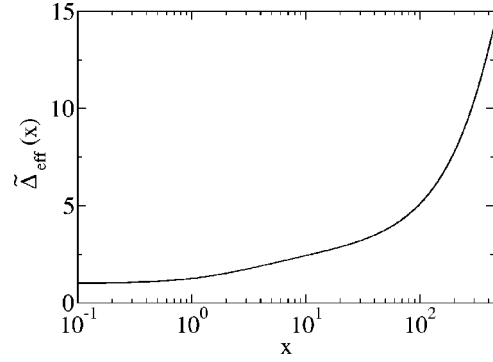


FIG. 1. The dimensionless effective hybridization function $\tilde{\Delta}_{\text{eff}}(x)$ evaluated for $\rho_0 J = 0.1$ in the Kondo model. The resulting function is symmetric and is only plotted for $x > 0$. It coincides with the universal form for $x \lesssim 30$. The fit (14) is indistinguishable from this line. Notice especially the appearance of logarithmic behavior in the crossover region.

resonant-level model becomes better since this procedure manages to partly also take the logarithmic term in Eq. (5) into account.

The resulting effective hybridization function can be scaled into a dimensionless form with one dimensionful parameter $\Delta_{\text{eff}}^0 \propto T_K$,

$$\Delta_{\text{eff}}(\epsilon) = \Delta_{\text{eff}}^0 \tilde{\Delta}_{\text{eff}}(\epsilon/\Delta_{\text{eff}}^0). \quad (13)$$

$\tilde{\Delta}_{\text{eff}}(x)$ is a universal function in the Kondo limit ($\rho_0 J \rightarrow 0$). It is depicted in Fig. 1 for $\rho_0 J = 0.1$, and coincides with its universal form for $|x| \lesssim 30$ ($|\epsilon| \lesssim 60T_K$, i.e., this should be sufficient for most practical purposes²²). For larger energies the effective hybridization function begins to cross over into linear behavior with logarithmic corrections depending on the *bare* coupling $\rho_0 J$. The following function provides an excellent fit (see Fig. 1):

$$\begin{aligned} \tilde{\Delta}_{\text{eff}}(x) = & 1 + \frac{1}{2} a_1 \ln \left[1 + \left(\frac{x}{a_0} \right)^2 \right] \\ & + a_2 \left(\arctan \left| \frac{x}{a_0} \right| - \left| \frac{x}{a_0} \right| \right) \left(1 - \ln \left| \frac{x}{a_0} \right| \right) \end{aligned} \quad (14)$$

with the parameters from Table I.

A similar analysis based on the comparison of flow equations shows that the above mapping between the Kondo model and the noninteracting resonant-level model can be extended to the case of a Kondo Hamiltonian (1) with a nonvanishing local magnetic field h ,

$$H_{\text{SIKM}} + g \mu_B h S_z, \quad (15)$$

TABLE I. Result of the fit (14) to the effective hybridization $\tilde{\Delta}_{\text{eff}}(x)$.

a_0	a_1	a_2
0.829	0.536	0.00324

by setting $\epsilon_d = g\mu_B h$ in the resonant-level model. However, the mapping with the above effective hybridization function becomes less accurate for $g\mu_B |h| \gtrsim T_K$ due to the approximate nature of the flow-equation solutions (5)–(7). We will discuss this point in more detail below.

Summing up, as long as we are interested in static quantities in a local magnetic field smaller than approximately T_K and/or dynamical correlation functions for energies smaller than approximately $60T_K$, we can use the resonant-level model with the effective hybridization function (14) to describe the physics of the Kondo model in the small coupling limit. The only undetermined parameter in the resonant-level model is the energy scale Δ_{eff}^0 that explicitly depends on J . This overall energy scale is proportional to T_K . Notice that the nonperturbative behavior of this energy scale

$$T_K \propto e^{-1/\rho_0 J} \quad (16)$$

follows correctly from the original flow Eqs. (5)–(7), see Ref. 16.

C. Calculation of physical quantities

Once the mapping between the Kondo model (1) and the effective resonant-level model (8) has been established, one can readily calculate physical quantities for the Kondo model. One complication arises from the fact that operators of the original Kondo model have to be transformed by a unitary transformation analogous to Eq. (2). In the language of the effective resonant-level model they will thus in general correspond to more complicated many-particle operators. Since the intention of this paper is to demonstrate the potential of our mapping in a pedagogical setting, we will concentrate on two quantities that remain simple under these transformations: (i) the z component of the spin operator S_z , which becomes $S_z = d^\dagger d - 1/2$, and (ii) the Hamiltonian itself.

From the latter we obtain the internal energy $U_{\text{imp}} = \langle H - H_0 \rangle$ and the Sommerfeld coefficient, $\gamma_{\text{imp}}(h)$. A straightforward calculation in the noninteracting resonant-level model yields

$$\gamma_{\text{imp}}(h) = \frac{\pi^2 k_B^2}{3} \rho_d(0) [1 - \Lambda'(0)], \quad (17)$$

where $\Lambda'(\omega)$ denotes the derivative of

$$\Lambda(\omega) = \frac{1}{\pi} P \int d\epsilon \frac{\Delta_{\text{eff}}(\epsilon)}{\omega - \epsilon}$$

and $P \int \dots$ is the principal-value integral. Here $\rho_d(\epsilon)$ is the impurity orbital density of states of the resonant-level model,

$$\rho_d(\epsilon) = \frac{1}{\pi} \frac{\Delta_{\text{eff}}(\epsilon)}{[\epsilon - g\mu_B h - \Lambda(\epsilon)]^2 + \Delta_{\text{eff}}^2(\epsilon)}. \quad (18)$$

The result (17) for γ_{imp} has some interesting implications. First, because d^\dagger is connected to S_+ , it is apparent that the low-energy excitations in the system are controlled by spin degrees of freedom, a well-known feature of the Kondo

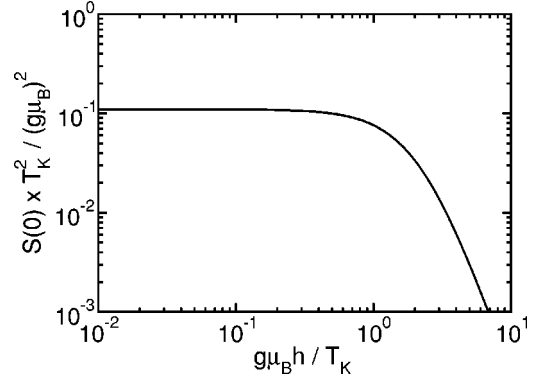


FIG. 2. Universal curve for $S(0)$ as a function of the local magnetic field h .

physics. However, in our approach this result can be read off directly from Eq. (17). Second, $\rho_d(0) \propto 1/\Delta_{\text{eff}}(0) \propto 1/T_K$, i.e., we obtain the correct scaling behavior for γ_{imp} directly from the behavior of $\Delta_{\text{eff}}(\epsilon)$. There is, however, a nontrivial correction coming from the factor in parentheses in Eq. (17). Note that for $\Delta_{\text{eff}}(\epsilon) = \text{const}$ this correction is one, but for the strongly ϵ dependent $\Delta_{\text{eff}}(\epsilon)$ in Fig. 1 it is of the order of two. As we will demonstrate later, this difference is directly responsible for obtaining the correct Wilson ratio in our approach.

From the mapping $S_z = d^\dagger d - 1/2$ it is easy to calculate $\chi_{zz}(\omega + i\delta) = -(g\mu_B)^2 \langle \langle d^\dagger d; d^\dagger d \rangle \rangle_{\omega + i\delta}$. Since the correlation function has to be evaluated within the resonant-level model, one obtains for the imaginary part at $T=0$

$$\chi''_{zz}(\omega) = (g\mu_B)^2 \pi \int_{-\omega}^0 d\omega' \rho_d(\omega') \rho_d(\omega + \omega'). \quad (19)$$

Again, this result provides direct access to an interpretation of the behavior of $\chi_{zz}(\omega + i\delta)$ in terms of the physics of the resonant-level model.

III. RESULTS

One quantity that can be calculated analytically is the low-energy limit of the spin-structure factor $S(\omega) \stackrel{\text{def}}{=} \chi''_{zz}(\omega)/\omega$,

$$S(0) = \lim_{\omega \rightarrow 0} \frac{\chi''_{zz}(\omega)}{\omega}. \quad (20)$$

For a vanishing local magnetic field, $S(0)$ is just the spin-relaxation rate accessible in, e.g., spin-resonance experiments. With the result for $\chi''_{zz}(\omega)$ from Eq. (19) we obtain

$$S(0) = (g\mu_B)^2 \frac{1}{\pi} \frac{\Delta_{\text{eff}}^2(0)}{[(g\mu_B h)^2 + \Delta_{\text{eff}}^2(0)]^2}, \quad (21)$$

which leads to the curve shown in Fig. 2. Equation (21) is of particular importance because it explicitly demonstrates universality, $T_K^2 S(\omega) = f(g\mu_B h/T_K)$, and allows to directly fit, e.g., experimental data from electron-spin-resonance or NMR experiments and extract the Kondo temperature. Note

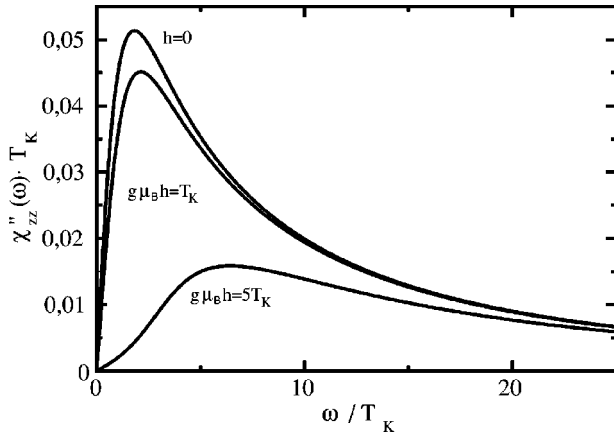


FIG. 3. $\chi''_{zz}(\omega)$ for three characteristic local magnetic fields $h=0$, $g\mu_B h = T_K$, and $g\mu_B h = 5T_K$.

furthermore that the result (21) is not only valid in the Kondo limit, but also holds at the Toulouse point of the anisotropic Kondo model and everywhere in between. Since it does not depend on the details of $\Delta_{\text{eff}}(\epsilon)$ it will also be true for general band structures $\epsilon_{\vec{k}}$ in Eq. (1) and thus is eventually the result for $S(0)$ in DMFT calculations.

The full frequency dependent $\chi''_{zz}(\omega)$ has to be calculated numerically using the form of the effective hybridization function in Fig. 1. The results for three values of the external field, $h=0$, $g\mu_B h = T_K$, and $g\mu_B h = 5T_K$, are displayed in Fig. 3. These correlation functions provide a good example for the usefulness of our mapping to the effective resonant-level model since one can directly interpret the structures and their frequency and field dependencies in terms of analytical formulas derived for the resonant-level model. For example, the high-frequency behavior of $\chi''_{zz}(\omega)$ follows directly from Eq. (19) and the behavior of the effective hybridization function $\Delta_{\text{eff}}(\epsilon)$ at large energies (which is linear with logarithmic corrections, see Fig. 1): $\chi''_{zz}(\omega)$ decays like $1/\omega$ with logarithmic corrections, in agreement with (expensive) numerical results.²³

For the dependence of the dynamical susceptibility on the local magnetic field one makes use of the fact that the local magnetic field corresponds to the on-site energy in the effective resonant-level model. Therefore it is obvious that the observed shift of the resonance peak in $\chi''_{zz}(\omega)$ is due to the shifted center of the resonant level. Furthermore, the depletion of the maximum value is related to the decreasing occupation of the resonant level, which corresponds directly to the *increasing* local magnetization in the Kondo model. At the same time, one observes a decrease of the total spectral weight in $\chi''_{zz}(\omega)$, which can be accounted for by a transfer to a finite expectation value of $\langle S_z \rangle$ in the Kondo model. There is, however, also a nontrivial effect, namely, the increasing broadening of the resonance peak with increasing magnetic field. For a resonant-level model with a constant $\Delta_{\text{eff}}(\epsilon)$ such a behavior does not occur; it is entirely related to the fact that with increasing magnetic field the system starts to notice the energy dependence of the effective hybridization.

The quantity not yet fixed in our calculation is T_K , or

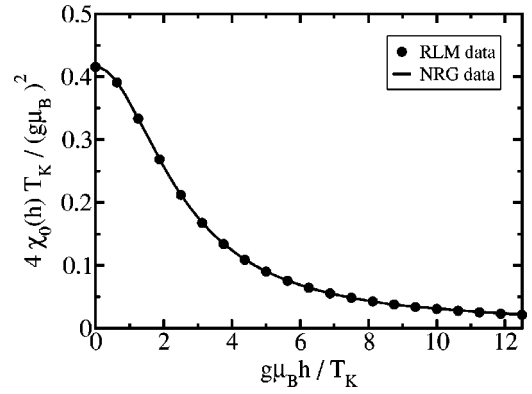


FIG. 4. The magnetic susceptibility $\chi_0(h)$ from Eq. (23) (circles) and the same quantity obtained from an NRG calculation.

more precisely the proportionality constant in $T_K \propto \Delta_{\text{eff}}(0)$. This can most conveniently be done by using Wilson's definition of the Kondo temperature³

$$\chi_0(h=0) = (g\mu_B)^2 \frac{w}{4T_K}, \quad (22)$$

where χ_0 is the static magnetic susceptibility and $w=0.413$ the Wilson number. χ_0 can be obtained from the imaginary part of the dynamic susceptibility (19) via

$$\chi_0 = \frac{2}{\pi} \int_0^\infty d\omega \frac{\chi''_{zz}(\omega)}{\omega} \quad (23)$$

and must in general be evaluated numerically. At the Toulouse point one can, however, give an analytic answer since $\Delta_{\text{eff}}(\omega) = \text{const}$ and thus

$$\chi_0(h) = (g\mu_B)^2 \frac{1}{\pi} \frac{\Delta_{\text{eff}}(0)}{h^2 + \Delta_{\text{eff}}(0)^2}. \quad (24)$$

Therefore at the Toulouse point the Korrington-Shiba relation²⁴

$$R_S = \frac{(g\mu_B)^2}{2\pi\chi_0^2} \lim_{\omega \rightarrow 0} \frac{\chi''_{zz}(\omega)}{\omega} \quad (25)$$

is independent of the local magnetic field

$$R_S = \frac{(g\mu_B)^2 S(0)}{2\pi\chi_0^2(h)} = \frac{1}{2}. \quad (26)$$

In the following we discuss $\chi_0(h)$ and the Korrington-Shiba relation for the Kondo limit $\rho_0 J \rightarrow 0$. The quantity $\chi_0(h)$ is particularly convenient for a comparison with NRG results. In Fig. 4 the circles represent the values of $\chi_0(h)$ calculated via Eq. (23) with the effective hybridization function from Fig. 1, and the full line represents the result of an NRG calculation. We observe excellent agreement for all values of the local magnetic field: notice that the curves agree without fit parameters. This example clearly demonstrates that the nontrivial form of the effective hybridization in Fig. 1 encodes the many-particle physics of the Kondo model in a trivial noninteracting effective model.

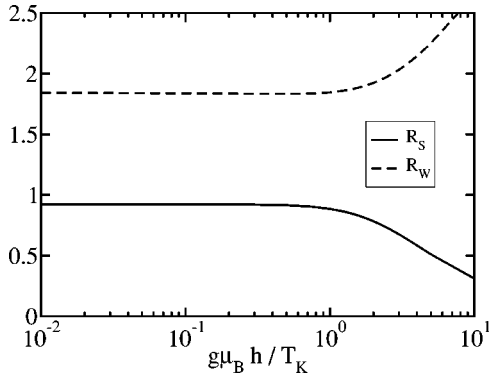


FIG. 5. Results for the Shiba ratio R_S (full line) and the Wilson ratio R_W (dashed line) as a function of a local magnetic field. The correct limiting values at $h \rightarrow 0$ are missed by approximately 5%.

The result in Fig. 4 can readily be combined with relations (17) and (21) to obtain the Wilson ratio⁵

$$R_W = \frac{4 \pi^2 k_B^2}{3 (g \mu_B)^2} \frac{\chi_{\text{imp}}(h)}{\gamma_{\text{imp}}(h)}. \quad (27)$$

From Eqs. (17) and (24) one immediately derives the well-known result $R_W(h) = 4$ on the Toulouse line independent of the magnetic field, which is twice the value in the small coupling Kondo limit.

Our results for the Wilson ratio and the Korringa-Shiba relation obtained within the effective resonant-level model describing the weak-coupling limit $\rho_0 J \rightarrow 0$ are collected in Fig. 5. For the Wilson ratio we would actually have to calculate the quantity χ_{imp} and not χ_0 .⁵ However, for the case of small $\rho_0 J$ considered here, both quantities are equivalent.²⁵ One observes that both R_W and R_S are independent of the local magnetic field up to approximately $g \mu_B h \approx T_K$, and then they start to decrease (Shiba ratio), respectively, and increase (Wilson ratio). The exact Bethe ansatz solution⁴ gives $R_W(h) = 2$ independent of the magnetic-field strength (see also Ref. 12), and local Fermi-liquid theory yields $R_S = 1$ for $h \rightarrow 0$.³ Our limiting values as $h \rightarrow 0$ miss these exact results by approximately 5%. Notice that the term $[1 - \Lambda'(0)]$ in Eq. (17) is very important to obtain this correct value for $R_W(h=0)$ because it reduces the Wilson ratio from the Toulouse line value to the value in the Kondo limit. Remarkably, our simple *noninteracting* effective model therefore correctly describes the Wilson ratio in the Kondo limit (for not too large magnetic fields), which is a hallmark of strong-coupling Kondo physics.

Let us finally analyze the accuracy of our effective model. Since Fig. 4 demonstrates that integral quantities such as $\chi_0(h)$ are obtained with very good accuracy for *all* magnetic fields, one can infer from Fig. 5 that quantities depending on low-energy details in frequency space such as γ_{imp} and $S(0)$ are more susceptible to our approximations for increasing magnetic fields. This suggests that for such low-energy quantities our effective model can be employed with very good accuracy (5% error) for magnetic fields below T_K , and with good accuracy (20% error) still up to approximately $5T_K$.

IV. SUMMARY AND OUTLOOK

Summing up, we have shown that the resonant-level model with a nontrivial hybridization function $\Delta_{\text{eff}}(\epsilon)$ can be used as an effective model for the single impurity Kondo model. The key observation was the fact that the flow-equation solutions of both models are approximately identical if a suitable $\Delta_{\text{eff}}(\epsilon)$ is chosen for the resonant-level model (Fig. 1). In this mapping the impurity orbital occupation number, $n_d - 1/2$ plays the role of the Kondo impurity spin S_z . The impurity orbital energy corresponds to the local magnetic field acting on S_z .

In contrast to the conventional approach where effective models describe the vicinity of the low-energy renormalization-group fixed points,^{3,5} our effective model very accurately describes both certain low- and high-energy properties of the original Kondo model: compare, for example, our discussion of the dynamical spin-spin correlation function in Fig. 3. It also yields thermodynamic quantities that are in excellent agreement with much more expensive numerical methods (see Fig. 4). The nontrivial behavior of the effective hybridization function encodes the quasiparticle interaction, which leads to, e.g., the correct Wilson ratio for small magnetic fields (with 5% accuracy).

In general, the evaluation of physical observables in the flow-equation approach requires following the flow of the operator under the infinitesimal unitary transformations (Sec. II C). Approximations and the ensuing accuracy of these transformations need to be studied on a case-by-case basis: it has been demonstrated above that thermodynamical quantities and the S_z - S_z correlation function can be evaluated very accurately. Likewise the spectral density and spin-density correlation functions with or without external magnetic field can be described very well within our effective model.²⁰ Other physical observables related to the conduction-band electron dynamics such as the T matrix or the conductivity have more complicated transformation properties under the infinitesimal unitary transformations and they will be investigated in a future publication.

In conclusion, our approach describes many aspects of the complicated many-body Kondo physics for not too large magnetic fields within a simple noninteracting model. Therefore one can very easily and intuitively understand certain properties of the Kondo model, e.g., the dependence of spin-spin correlation functions on a local magnetic field (Fig. 3). One main prospect of our approach is to look at other correlation functions using this effective model, in particular, the T matrix for applications in the framework of DMFT calculations. Future prospects also include cluster problems and the single impurity Anderson model. Work along these lines is in progress.

ACKNOWLEDGMENTS

We acknowledge valuable conversations with N. Andrei, R. Bulla, W. Hofstetter, D. Logan, A. Rosch, M. Vojta, and D. Vollhardt. This work was supported by the DFG collaborative research center SFB 484 and NSF Grant No. DMR-0073308.

- ¹J. Kondo, *Prog. Theor. Phys.* **32**, 27 (1964).
- ²P. W. Anderson, *Phys. Rev.* **124**, 41 (1961).
- ³For a comprehensive overview see, e.g., A. C. Hewson, *The Kondo Problem to Heavy Fermions* (Cambridge University, Cambridge, England, 1993).
- ⁴N. Andrei, K. Furuya, and J. H. Lowenstein, *Rev. Mod. Phys.* **55**, 331 (1983); A. M. Tselick and P. B. Wiegmann, *Adv. Phys.* **32**, 453 (1983).
- ⁵K. G. Wilson, *Rev. Mod. Phys.* **47**, 773 (1975); H. R. Krishnamurthy, J. W. Wilkins, and K. G. Wilson, *Phys. Rev. B* **21**, 1003 (1980); **21**, 1044 (1980).
- ⁶J. E. Hirsch and R. M. Fye, *Phys. Rev. Lett.* **56**, 2521 (1986).
- ⁷M. Jarrell and J. E. Gubernatis, *Phys. Rep.* **269**, 135 (1996).
- ⁸T. Costi, *Phys. Rev. Lett.* **85**, 1504 (2000).
- ⁹M. T. Glossop and D. E. Logan, *J. Phys.: Condens. Matter* **13**, 9713 (2002).
- ¹⁰D. E. Logan, M. P. Eastwood, and M. A. Tusch, *J. Phys.: Condens. Matter* **10**, 2673 (1998); D. E. Logan and M. T. Glossop, *ibid.* **12**, 985 (2000).
- ¹¹R. Bulla, M. T. Glossop, D. E. Logan, and Th. Pruschke, *J. Phys.: Condens. Matter* **12**, 4899 (1998).
- ¹²D. E. Logan and N. L. Dickens, *Europhys. Lett.* **54**, 227 (2001).
- ¹³W. Metzner and D. Vollhardt, *Phys. Rev. Lett.* **62**, 324 (1989); A. Georges, G. Kotliar, W. Krauth, and M. J. Rozenberg, *Rev. Mod. Phys.* **68**, 13 (1996).
- ¹⁴F. Wegner, *Ann. Phys. (Leipzig)* **3**, 77 (1994).
- ¹⁵S. Kehrein, *Phys. Rev. Lett.* **83**, 4914 (1999); S. Kehrein, *Nucl. Phys. B* **592**, 512 (2001).
- ¹⁶W. Hofstetter and S. Kehrein, *Phys. Rev. B* **63**, 140402(R) (2001).
- ¹⁷G. Toulouse, *C. R. Acad. Sci. III* **268**, 1200 (1969).
- ¹⁸For an overview of bosonization and refermionization techniques see, e.g., J. von Delft and H. Schoeller, *Ann. Phys. (Leipzig)* **7**, 225 (1998).
- ¹⁹The investigation of nontrivial dispersion relations is one of the main future perspectives of the flow-equation approach. Work along these lines is in progress.
- ²⁰S. Kehrein (unpublished).
- ²¹S. Kehrein and A. Mielke, *Ann. Phys. (N.Y.)* **252**, 1 (1996).
- ²²It becomes increasingly difficult to numerically investigate smaller couplings.
- ²³T. A. Costi and C. Kieffer, *Phys. Rev. Lett.* **76**, 1683 (1996).
- ²⁴H. Shiba, *Prog. Theor. Phys.* **54**, 967 (1975).
- ²⁵K. Chen, C. Jayaprakash, and H. R. Krishnamurthy, *Phys. Rev. B* **45**, 5368 (1992).